

UNLOCKING THE POWER OF CO-OCCURRENCE IN CLIP: A DUALPROMPT-DRIVEN METHOD FOR TRAINING-FREE ZERO-SHOT MULTI-LABEL CLASSIFICATION

Anonymous authors

Paper under double-blind review

ABSTRACT

Contrastive Language-Image Pretraining (CLIP) has exhibited powerful zero-shot capacity in various single-label image classification tasks. However, when applying to the multi-label scenarios, CLIP suffers from significant performance declines due to the lack of explicit exploitation of co-occurrence information. In pretraining, due to the contrastive property of its used objective, the model focuses on the prominent object in an image, while overlooking other objects and their co-occurrence relationships; in inference, it uses a discriminative prompt containing only a target label name to make predictions, which does not introduce any co-occurrence information. Then, an important question is as follows: *Do we need label co-occurrence in CLIP for achieving effective zero-shot multi-label learning?* In this paper, we propose to rewrite the original prompt into a correlative form consisting of both the target label and its co-occurring labels. An interesting finding is that such a simple modification can effectively introduce co-occurrence information into CLIP and it exhibits both good and bad effects. On the one hand, it can enhance the recognition capacity of CLIP by exploiting the correlative pattern activated by the correlative prompt; on the other hand, it leads to object hallucination in CLIP, where the model predicts objects that do not actually exist in the image, due to overfitting to co-occurrence. To address this problem, we proposed to calibrate CLIP predictions by keeping the positive effect while removing the negative effect caused by suspicious co-occurrence. **This can be achieved by using dual prompts consisting of the discriminative and correlative prompts, which introduce label co-occurrence while emphasizing the discriminative pattern of the target object.** Experimental results verify that our method can achieve better performance than the state-of-the-art methods.

1 INTRODUCTION

Vision-Language Models (VLMs) trained on massive cheaply collected data have demonstrated immense potential in many realistic tasks, *e.g.*, object detection (Gu et al., 2022), semantic segmentation Lin et al. (2023), and anomaly detection (Zhou et al., 2024). As a representative model, CLIP performs pretraining by aligning large-scale image-text using a contrastive objective, showing strong zero-shot generalization ability in various downstream tasks. To perform zero-shot image classification, a vanilla strategy is to expand each label name with a set of prompt templates, *e.g.*, “A photo of a {label}”, showing impressive zero-shot classification performance in many benchmark datasets Radford et al. (2021). Although CLIP has achieved successes in the single-label zero-shot classification tasks, it often suffers from unfavorable performance when applied to more realistic multi-label scenarios, where an image is often associated with multiple labels.

There are two major challenges in achieving effective zero-shot multi-label classification. As pointed by (Lin et al., 2024), the first challenge is that CLIP tends to capture the global features of an entire image dominated by the most prominent object, while neglecting the local features of others. This limits its ability to recognize multiple objects simultaneously, often leading to the precise recognition of only the most prominent object while overlooking others. To address this, TagCLIP (Lin et al.,

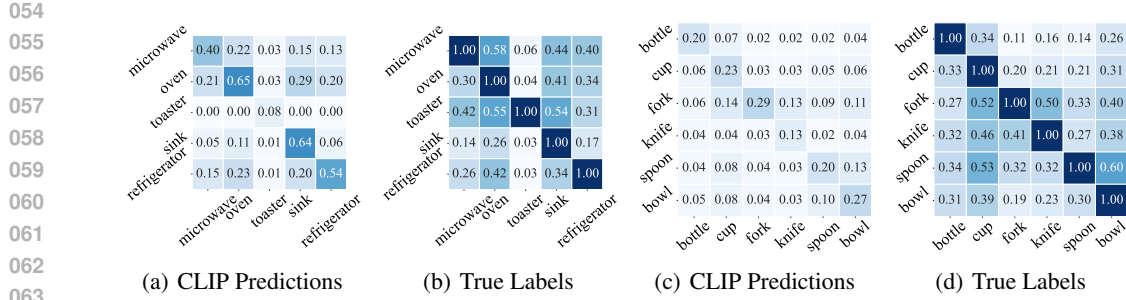


Figure 1: The co-occurrence probabilities of CLIP predictions and true labels. Without explicitly exploiting label correlations, CLIP is hard to precisely model the co-occurrence among labels.

2024) adopted the Vision Transformer (ViT) (Dosovitskiy et al., 2021) as the backbone of CLIP to explore the local features of patches, which are usually useful for identifying inconspicuous objects. However, one limitation of this method lies in its heavy reliance on ViT to obtain local features of patches for performing classification, which reduces its universality and prevents it from being applied to other backbones, *e.g.*, ResNet (He et al., 2016).

The other challenge is that CLIP does not explicitly leverage label correlations, *i.e.*, co-occurrence relationships, during both pretraining and inference, which has been proven to be indispensable for multi-label classification Chen et al. (2019); Lanchantin et al. (2021). In pretraining, the contrastive objective used in CLIP leads its image encoder to focus on the prominent object in an image (Lin et al., 2024), while neglecting others and their co-occurrence patterns; in inference, using a discriminative prompt such as “A photo of a {label}” does not introduce any co-occurrence information. To verify this, we perform zero-shot multi-label classification on benchmark dataset, MS-COCO Lin et al. (2014), and show the co-occurrence probabilities of vanilla CLIP predictions and true labels in Figure 1. Considering that it is too large to display the entire matrix in the main text, we select two subsets of frequently co-occurring objects and show their co-occurrence probabilities. From the figure, there is a significant gap between the estimated co-occurrence probabilities and the true ones, which means that vanilla CLIP cannot precisely model co-occurrence relationships. This indicates that it cannot effectively reduce the complexity of the output space by capturing prior information of label relationships, which often leads to missing labels and consequently degrades model performance. An important question has emerged: *Do we need label co-occurrence in CLIP to achieve effective zero-shot multi-label classification?*

In this paper, unlike the previous work that focuses on enhancing image feature representation, we propose to rewrite the original discriminative prompt and obtain a correlative prompt for each target label by including its co-occurring labels. An interesting finding is that such a simple modification effectively introduces co-occurrence information, prompting the model to capture co-occurrence patterns, which enhances its ability to recognize multiple objects. Unfortunately, we find that CLIP tends to overfit to the co-occurrence relationships introduced by the correlative prompts. This leads the model to suffer from an object hallucination issue, where it makes predictions even when the target object does not exist in the image while its co-occurring objects do. To address this problem, inspired by the recent study (Xie et al., 2024), we build a causal inference framework by modeling the co-occurrence as a mediator. This enables us to calibrate the CLIP predictions by removing the biased prediction caused by mediated effect from the prompt of co-occurring labels to target prediction. In practical implementation, our derivation shows that this can be achieved simply by combining the outputs of the discriminative prompt and the correlative prompt. Comprehensive experimental results verify that our method can achieve better performance than the state-of-the-art methods.

2 RELATED WORKS

106 Multi-label image classification aims to train a multi-label classifier that can predict all relevant labels for unseen images. The pioneering work (Wang et al., 2016) combined Convolutional Neural Networks (CNNs) and Recurrent Neural Networks (RNNs) and developed CNN-RNN framework

108 to characterize the label correlations as well as the image-label relevance. To address the issue that
 109 dataset-level statistical correlations may not hold for every individual image, Structured Semantic
 110 Transfer (SST) (Chen et al., 2022) introduced the Intra-image Semantic Transfer (IST) mod-
 111 ule, which learns an image-specific co-occurrence matrix and leverages this information to recover
 112 unknown labels. To overcome the challenge that incomplete annotations make it difficult to esti-
 113 mate label co-occurrence, SCPNet (Ding et al., 2023) computed text features by feeding category
 114 names into the CLIP text encoder, and uses their pairwise similarities as a surrogate for the label
 115 co-occurrence. Zhang et al. (2024) developed a large model to achieve the goal of recognizing any
 116 object. Yue et al. (2024) treated the task of object recognition as the task of next token prediction.
 117

118 Prompt tuning (Zhou et al., 2022) learns continuous vectors as task-specific prompts based on a
 119 small number of training examples. The idea has been applied to multi-label image classification
 120 and achieved impressive performance (Sun et al., 2022; Hu et al., 2023). Given that images may
 121 be costly to collect while texts are cheap to generate, Guo et al. (2023) proposed Texts as Images
 122 in prompt tuning (TaI) to adapt CLIP to multi-label image classification based on only the textual
 123 modality.

124 3 PRELIMINARIES

126 In our setting, the task is to perform multi-label image classification, also known as object recogni-
 127 tion Yue et al. (2024) or image tagging Zhang et al. (2024), using CLIP without training. Specifically,
 128 we are given a dataset $\{\mathbf{x}_i\}_{i=1}^n$ consisting of n test instances. Each instance is associated with an
 129 unknown label vector $\mathbf{y}_i \subseteq \mathcal{Y}$, where $\mathcal{Y} = \{0, 1\}^q$ is the label space with q possible class labels.
 130 Here, $y_k = 1$ indicates that the k -th label is relevant while $y_k = 0$ indicates that it is not. Our
 131 task is to develop an inference strategy that enables CLIP to accurately predict all relevant labels for
 132 each test instance. We begin with a brief introduction of CLIP. We use $[q]$ to denote the integer set
 133 $\{1, \dots, q\}$.

134 CLIP consists of an image encoder $\text{Enc}_I(\cdot)$ and a text encoder $\text{Enc}_T(\cdot)$. To perform zero-shot classi-
 135 fication, a conventional method is to construct a prompt P_k using a template like “A photo of a
 136 {label}_ k ”, where label_k is the name of the k -th label. By using these two encoders, the image
 137 and text features can be obtain as

$$138 \quad \mathbf{f}_i = \text{Enc}_I(\mathbf{x}_i), \quad \mathbf{t}_k = \text{Enc}_T(P_k), \forall k \in [q].$$

139 Then, by computing the cosine similarity between the image features \mathbf{f}_i and the text features \mathbf{t}_k and
 140 applying the softmax activation function, we obtain the predicted probabilities as
 141

$$142 \quad p(y_k = 1 | \mathbf{x}_i, P_k) = \frac{\exp(\langle \mathbf{f}_i, \mathbf{t}_k \rangle)}{\sum_{k=1}^q \exp(\langle \mathbf{f}_i, \mathbf{t}_k \rangle)}, \forall k \in [q],$$

144 where $\langle \cdot, \cdot \rangle$ denotes the cosine similarity.
 145

146 The original paper of CLIP has shown that prompt engineering and ensembling can enhance the
 147 performance of its zero-shot classification (Radford et al., 2021). For example, the original sin-
 148 gle prompt can be expanded into a set of prompts by including prompts such as “A satellite
 149 photo of a {label}” and “A photo of a big {label}”.

151 4 DO WE NEED CO-OCCURRENCE IN CLIP?

153 As discussed before, a potential limitation of CLIP is that it does not explicitly exploit co-occurrence
 154 information during either the pretraining phase or the inference phase. Co-occurrence information
 155 has long been proven to significantly enhance multi-label classification performance (Chen et al.,
 156 2019). Consequently, an important question arises: *Do we need co-occurrence in CLIP for zero-
 157 shot multi-label classification?* To answer this question, we perform experiments on MS-COCO by
 158 incorporating co-occurrence information during the inference phase.

159 Specifically, for each label y_k with the name label_k , we assume that there is a set of co-occurring
 160 labels $\mathcal{C}_k = \{\text{label}_j\}_{j=1}^{m_k}$, where m_k is the number of co-occurring labels for the label y_k . We
 161 will discuss how to obtain the co-occurring label set in the latter section. Then we rewrite the
 prompt as “A photo of a {label}_ k often includes a {label}_ 1 , ..., a {label}_ m_k ”.

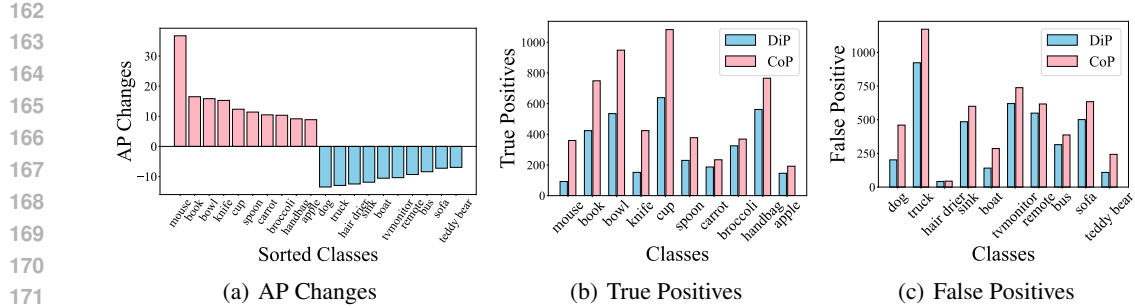


Figure 2: Empirical Validations on the advantages and disadvantages of CoP. (a) shows top 10 performance improvements and top 10 performance declines after using CoP. (b) shows the co-occurrence probabilities of CLIP predictions using CoP. (c) reports the number of **false positives** that contains co-occurring objects predicted by DiP and CoP.

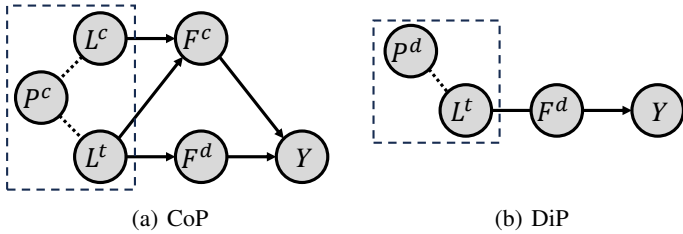


Figure 3: The causal graphs of DiP and CoP. P^d and P^c are the discriminative and correlative prompts. F^d and F^c are the discriminative and correlative features. Y is the prediction of the target label.

This allows us to introduce co-occurrence information into CLIP inference through prompts. We refer to this prompt as the Correlative Prompt (CoP), while referring to the original prompt as the Discriminative Prompt (DiP). Figure 2(a) illustrates the performance improvements/declines of CoP over DiP, sorted by the performance changes in terms of commonly used Average Precision (AP). As shown in the figure, some labels experienced significant performance improvements, while others saw substantial declines. Due to the page limit, we only show the top-10 labels with the highest performance improvements and the top-10 with the greatest performance declines. The complete results can be found in Appendix B. To disclose the reason why the improvements are achieved on these labels, we report the number of true positive instances that contain the target label and its co-occurring labels, measuring how large co-occurrence helps the model to identify the target object. The metric measures the positive impact of co-occurrence on the CLIP predictions. Obviously, CoP makes far more correct predictions than DiP on most of these labels. This indicates that co-occurrence is useful for enhancing CLIP’s ability to recognize multiple objects.

In Figure 2(a), we also present top-10 labels with the greatest performance declines achieved by CoP. To provide an explanation for this phenomenon, for each target label, Figure 2(c) illustrates the number of false positive instances that contain its co-occurring labels, measuring how many incorrect predictions are caused by the model’s overfitting to co-occurrence. It is obvious to see that CoP makes far more incorrect predictions caused by the overfitting issue than DiP in almost all labels. While CoP benefits from co-occurrence information, it still carries the risk of overfitting to it.

A Causal Perspective To provide a theoretical explanation of these phenomena, as shown in Figure 3(a), we construct a causal inference framework to show how CoP leverages co-occurrence information. The framework includes three kinds of variables: the correlative prompt P^c consisting of the target label L^t and its co-occurring labels L^c , the discriminative activated features F^d and the correlative activated features F^c , and the model prediction Y for the target label. We use \rightarrow to represent the causal link between any two variables, which indicates their causal effects. For the

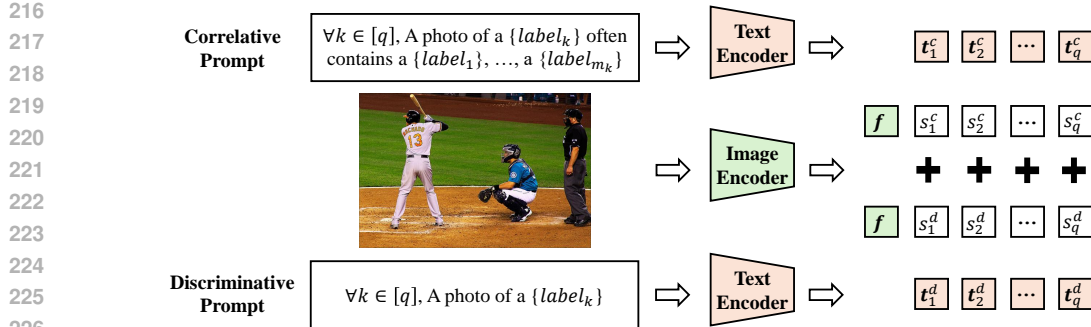


Figure 4: The framework of DualPrompt. It consists of two types of prompts. The correlative prompt is used to maintain the good causal effect of co-occurrence by exploring correlative patterns, while the discriminative prompt is used to remove the bad causal effect by enhancing the discriminative responses.

sake of comparison, Figure 3(b) shows the causal graph of DiP, where P^d represents the discriminative prompt only containing the target label L^t . On the one hand, compared to DiP, which can only make predictions by activating the discriminative features through the single path $L^t \rightarrow F^d \rightarrow Y$, CoP can still make predictions by activating the correlative features through an additional path $(L^t, L^c) \rightarrow F^c \rightarrow Y$, especially when the former does not work. This improves CLIP’s ability to recognize inconspicuous objects by leveraging co-occurrence information, which is verified by the results in Figure 2(b). On the other hand, we consider a case where the target object does not exist in an image but its co-occurring objects do. The discriminative features would not be activated by the target label L_t in the correlative prompt, *i.e.*, the path $L^t \rightarrow F^d \rightarrow Y$ is disconnected, due to the fact that there is no target object; while the correlative features would be activated by the co-occurring labels L^c in the correlative prompt, *i.e.*, the path $L^c \rightarrow F^c \rightarrow Y$ is connected, due to the fact that there exist co-occurring objects. This enables the model to give a high probability of the target object that does not even exist, which can be supported by the results in Figure 2(c). The above discussions tell us that co-occurrence has not only a positive side: it enhances the CLIP’s ability to identify the target objects, but also a negative side: it makes CLIP suffer from the overfitting issue and cause object hallucination (Biten et al., 2022). The important question now becomes: *Can we keep the positive side while mitigating the negative side of co-occurrence in CLIP?*

5 UNLOCKING THE POWER OF CO-OCCURRENCE

For CoP, the predicted probability can be written as $p(y_k = 1 | \mathbf{x}_i, P_k^c)$ or $p(y_k = 1 | \mathbf{x}_i, L_k^t, L_k^c)$, where P_k^c is the correlative prompt consisting of the target label L_k^t and its co-occurring labels L_k^c for the k -th class. However, when there are only co-occurring objects in an image and no target object, CLIP still activates the correlative features by the co-occurring labels in the **prompt** through the path $L^c \rightarrow F^c \rightarrow Y$ and gives a high probability of the target object. This indicates that CLIP suffers from overfitting to the co-occurrence, leading to object hallucination. To address this problem, we propose to calibrate the CoP prediction via the total direct effect (TDE) (Pearl, 2001), with the goal of removing the biased part of the prediction. For a given image \mathbf{x} , we define the TDE prediction with respect to the k -th class as

$$\mathcal{T}_k(\mathbf{x}) = p(y_k = 1 | \mathbf{x}, L_k^t, L_k^c) - p(y_k = 1 | \mathbf{x}, L_k^c). \quad (1)$$

The first term represents the positive causal effect, where CLIP makes a prediction based on the target label prompt L^t and its co-occurring label prompt L^c ; the second term represents the negative effect, where CLIP makes a prediction based on only the co-occurring label prompt. The minus sign indicates that we keep the positive effect while discarding the negative effect.

However, in our experiments, we find Eq. (1) hardly works. This may be because CLIP often overestimates the probability $p(y_k = 1 | \mathbf{x}, L_k^c)$, especially when some labels preferred by CLIP appear in L^c . This leads the final predictions to underestimation, resulting in performance declines. To address this problem, we derive an equivalent form of Eq. (1), which transforms it from a subtraction

270
 271 Table 1: The comparative results between the proposed method and the state-of-the-art methods on
 272 MS-COCO dataset. The best performance is highlighted in bold. Coo. Est. represents co-occurrence
 273 probabilities estimation.

	Backbone	Resolution	Training Data Usage	mAP	F1
DualCoOp	ResNet-101	224 × 224	1% Data for Training	56.3	55.1
TaICLIP	ResNet-101	224 × 224	1% Data for Training	56.6	55.7
TaICLIP	ResNet-101	224 × 224	COCO Captions	65.1	–
CLIP	ResNet-101	224 × 224	None	62.9	59.8
DualPrompt	ResNet-101	224 × 224	None	65.5	61.7
DualPrompt	ResNet-101	224 × 224	1% Data for Coo. Est.	67.1	63.0
DualCoOp	ViT-B/16	224 × 224	1% Data for training	55.1	54.4
TaICLIP	ViT-B/16	224 × 224	1% Data for training	63.6	55.9
CLIP	ViT-B/16	224 × 224	None	64.9	61.5
DualPrompt	ViT-B/16	224 × 224	None	67.7	63.6
DualPrompt	ViT-B/16	224 × 224	1% Data for Coo. Est.	69.4	65.0
TagCLIP	ViT-B/16	Original	None	68.7	65.2
DualPrompt + TagCLIP	ViT-B/16	Original	None	69.2	65.4
DualPrompt + TagCLIP	ViT-B/16	Original	1% Data for Coo. Est.	70.0	66.1

291
 292 form into an addition form as ¹
 293

$$T_k(\mathbf{x}) = p(y_k = 1|\mathbf{x}, P_k^c) + p(y_k = 1|\mathbf{x}, P_k^d). \quad (2)$$

294 The second term represents the direct causal effect, where CLIP makes a prediction based on the
 295 discriminative prompt P^d containing only the target label L^t . The plus sign indicates that we en-
 296 hance the direct effect. An intuitive explanation of this transformation is that mitigating the indirect
 297 effect is equivalent to strengthening the direct effect. We refer to this method as DualPrompt.

300 Figure 4 provides an illustration of our proposed DualPrompt method. Unlike the vanilla method, the
 301 bottom branch, which uses the discriminative prompt, our DualPrompt method uses dual prompts,
 302 a discriminative prompt and a correlative prompt, to achieve effective zero-shot multi-label classi-
 303 cation.

304
 305 **How to Obtain Co-Occurrence?** Considering that co-occurrence has both universality, meaning
 306 that it is a natural law used to describe the physical world, and specificity, meaning that it may
 307 vary across different datasets, we employ two methods to obtain co-occurrence information in ex-
 308 periments. Firstly, we ask ChatGPT-4o to generate up to l labels that frequently appear with target
 309 objects in the same images. We find that the co-occurring labels generated by ChatGPT are not
 310 completely correct. A large l often means that more labels without co-occurrence relationships are
 311 introduced, which can mislead the model and result in performance declines. To avoid this problem,
 312 we set l to be as small as 2 in our experiments. The other method is to annotate a tiny amount of train-
 313 ing data and only use it for estimating the co-occurrence probabilities. The most co-occurring labels
 314 for each target label can be found according to the co-occurrence probabilities. Our empirical stud-
 315 ies in Section 6 show that a very small number of examples, e.g., 1% training data in the MS-COCO
 316 dataset, are needed to obtain an acceptable co-occurrence probability, which are often insufficient to
 317 fine-tune CLIP by existing methods (Sun et al., 2022) to achieve favorable performance.

318 6 EXPERIMENTS

319 We first compare our proposed method with the state-of-the-art methods; then, we perform ablation
 320 studies to examine the contribution of each component.

321
 322 ¹The detailed derivation can be found in Appendix A.

324
 325 Table 2: The comparative results between the proposed method and the state-of-the-art methods on
 326 VG-256 dataset. The best performance is highlighted in bold. Coo. Est. represents co-occurrence
 327 probabilities estimation.

	Backbone	Resolution	Training Data Usage	mAP	F1
DualCoOp	ResNet-101	224 × 224	2% Data for Training	30.4	33.5
TaICLIP	ResNet-101	224 × 224	2% Data for Training	32.0	34.9
CLIP	ResNet-101	224 × 224	None	29.2	32.2
DualPrompt	ResNet-101	224 × 224	None	33.5	36.1
DualPrompt	ResNet-101	224 × 224	2% Data for Coo. Est.	35.2	37.6
TagCLIP	ViT-B/16	Original	None	39.6	41.9
DualPrompt + TagCLIP	ViT-B/16	Original	None	40.2	42.4
DualPrompt + TagCLIP	ViT-B/16	Original	2% Data for Coo. Est.	40.7	42.7

339 6.1 EXPERIMENTAL SETTINGS

340 **Dataset** To evaluate the performance of the proposed method, we perform experiments on two
 341 benchmark datasets, including MS-COCO 2014² (MS-COCO for short) (Lin et al., 2014) and Vi-
 342 sual Genome³ (Krishna et al., 2017). MS-COCO contains 82,081 training images and 40,137 val-
 343 idation images for 80 classes, with an average of 2.9 labels per image. Visual Genome is a dataset
 344 that contains 108,249 images from 80,138 categories. By performing preprocessing as done in the
 345 previous work (Xie et al., 2024), we obtain a dataset named VG-256 that contains 106,702 images
 346 and 256 classes. We randomly split the entire dataset into a 70% training set with 74,691 images
 347 and a 30% validation set with 32,011 images. We directly evaluate our method and other methods
 348 on the validation set. The commonly used mean Average Precision (mAP) and per-class F1 (F1)
 349 are used as the evaluation metrics. To ensure a fair comparison, we set the random seed to 1 for all
 350 experiments.

351 **Implementation** For CLIP, we use ResNet-101 (He et al., 2016) and ViT-B/16 (Dosovitskiy et al.,
 352 2021) as the backbones. For TagCLIP, we use the original resolution of images as done in its original
 353 paper; for other methods, we use a resolution of 224 × 224. Following the previous work (Lin et al.,
 354 2024), we use the 80 prompts used in CLIP (Radford et al., 2021). For prompt fine-tuning methods,
 355 when only 1% of the training data is available, the batch size is set to 16; when 2%-5% of the training
 356 data is available, the batch size is set to 32. The other parameters use the reference values provided
 357 in the original papers. All experiments were run on single NVIDIA A100 GPUs.

361 6.2 COMPARISON WITH STATE-OF-THE-ART METHODS

362 To validate the effectiveness of the proposed method, we compare it with two types of CLIP-based
 363 methods: i) two training-based methods, DualCoOp (Sun et al., 2022), which performs prompt
 364 tuning based on a subset of downstream training data, and TaI (Guo et al., 2023), which trains on a
 365 subset of data or curated caption data in the downstream task; ii) two training-free methods, CLIP
 366 (Radford et al., 2021) and TagCLIP (Lin et al., 2024).

367 Table 1 and Table 2 report the results of the proposed method and other methods on MS-COCO and
 368 VG-256, respectively. From the table, we can see that: i) DualPrompt outperforms both training-
 369 based and training-free methods with a significant margin. ii) By combining DualPrompt and Tag-
 370 CLIP, we achieve the state-of-the-art performance on both two datasets. iii) For the two methods
 371 of obtaining co-occurrence labels, it is evident that co-occurrence estimation with a tiny number of
 372 data is better than ChatGPT. The co-occurrence provided by ChatGPT is universally existing regu-
 373 larity, while co-occurrence estimation is based on the prior of the downstream dataset. These results
 374 convincingly verify that the proposed method can achieve the state-of-the-art performance.

375²<https://cocodataset.org>

376³<https://homes.cs.washington.edu/~ranjay/visualgenome/index.html>

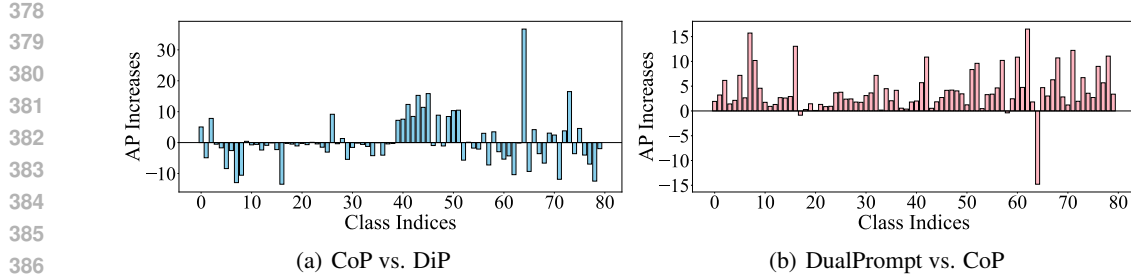


Figure 5: Comparisons of per-class average precision among DiP, CoP, and DualPrompt. Compared with DiP, CoP shows improvements on some categories but decreases on others, whereas compared with CoP, DualPrompt achieves improvements on the vast majority of categories.

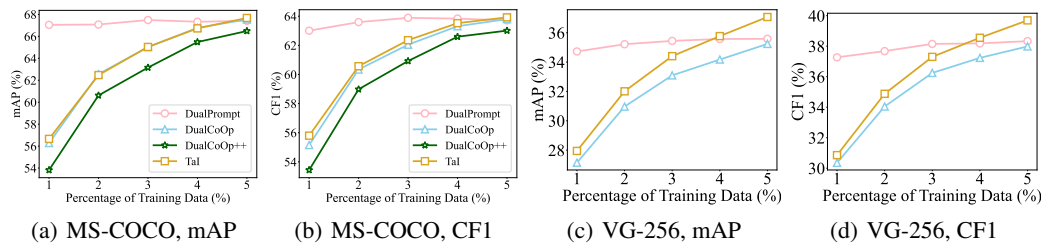


Figure 6: The performance curve with the increase of training data usage. For DualPrompt, training data is only used for estimating co-occurrence probabilities; while for DualCoOp, training data is used for model training.

6.3 ABLATION STUDIES

We provide empirical validations on how DualPrompt keeps the positive impact while removing the negative impact of co-occurrence. Figure 5 illustrates a stepwise evaluation on MS-COCO in terms of AP. From the figure, we can see that CoP achieves better performance than DiP on some classes, while performing worse on others. Overall, the performance of CoP is inferior to that of DiP. This is because CLIP overfits to the co-occurring labels given in the prompt, making many false positive predictions, which leads to a decline in model performance. To address this problem, our proposed method calibrates the predicted probabilities via TED measurement by removing the biased parts. DualPrompt achieves performance improvements in almost all classes, providing convincing evidence that it can maintain the positive effect while removing the negative effect.

6.4 STUDY ON TRAINING DATA USAGE

In our method, we need to obtain the co-occurring labels for each target label. A solution is to estimate the co-occurrence probabilities based on a very small subset of training data and obtain co-occurrence according to probabilities. In this subsection, we show that such a small number of training data is insufficient for model training. Figure 6 illustrates the performance curves of our method and prompt tuning methods, DualCoOp and TaI. It is noteworthy that our method only uses the training data for estimating co-occurrence probabilities, while DualCoOp and TaI use them for fine-tuning the model. From the figure, it can be observed that with a very small number of training (1%), there is a significant performance gap between our method and prompt tuning methods. With the increase of training data, the gap gradually narrows, and eventually, TaI outperforms our method. This indicates that our method requires such a small number of training data to estimate co-occurrence probabilities that they are not even sufficient for fine-tuning the model.

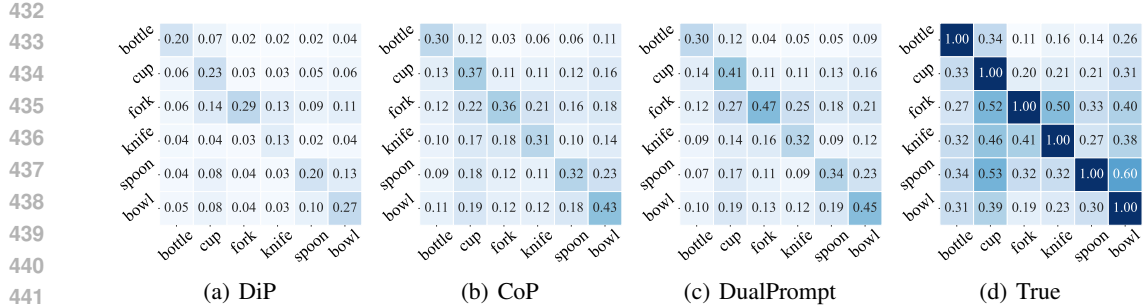


Figure 7: The co-occurrence probabilities of different predictions and true labels.

Figure 8: The text-image retrieval results of DiP (the first row), CoP (the second row) and DualPrompt (the last row) with respect to *cup* (on the left side) and *sink* (on the right side). To show the representativeness of different methods, we present the images ranked 1st, 5th, 10th, 15th, and 20th based on text-image similarities.

6.5 STUDY ON CO-OCCURRENCE ESTIMATION

In this subsection, we demonstrate the ability of different methods to capture co-occurrence relationships. Figure 7 illustrates the co-occurrence probabilities estimated by different methods in the *kitchenware* scenario consisting of six classes: *bottle*, *cup*, *fork*, *knife*, *spoon*, *bowl*. We can see that CoP performs better than DiP on some classes, while performing worse on others. This means that although CoP benefits from the advantage of correlative prompts, it still suffers from the overfitting to co-occurrence. Suspicious co-occurrence hinders further performance improvement. To address this problem, DualPrompt aims to remove the negative impact caused by suspicious co-occurrence and achieve better co-occurrence estimation than both DiP and CoP.

6.6 TEXT-IMAGE RETRIEVAL RESULTS

To explore the mechanism behind DualPrompt, as shown in Figure 8, we visualize some images according to text-image similarity scores. Three rows represent the text-image retrieval results of DiP, CoP and DualPrompt. For each method, we illustrate the images ranked 1st, 5th, 10th, 15th, and 20th according to similarity scores. From the figure, we can see that the retrieved images from different methods exhibit significant differences. DiP tends to retrieve the images dominated by the target object. It sometimes make a mistake due to the ambiguous object, *e.g.*, incorrectly identify a *vase* as a *cup* in the 15-th image. While CoP tends to retrieve images that depict scenes characterized by the target object and its co-occurring objects, such as a dining table full of plates or a fully equipped bathroom. This indicates that CoP identifies the target object by exploiting co-occurrence information. But it often suffers from the overfitting issue and make incorrect predictions based on only the co-occurring objects, *e.g.*, there is no *cup* but only its co-occurring objects like *bowl* and *bottle* in the 15-th image. The images retrieved by DualPrompt seem to be a combination of the first two methods. DualPrompt enhances the text-image matching ability by leveraging the advantages

486
487
488
489
490

491 Toaster Sink Refrigerator | Bottle Fork Knife

492

493 Figure 9: Object hallucination cases obtained by DualPrompt. The hallucinated category names are
494 shown below each image.

495

496
497
498

of the first two methods, which aims to identify the target object based on discriminative features and correlative patterns.

499
500

6.7 FAILURE CASE ANALYSIS

501
502
503
504
505
506
507
508
509

In this subsection, we present a failure case analysis of DualPrompt in addressing the overfitting issue caused by label co-occurrence. Figure 9 shows cases where DualPrompt produces object hallucinations on two groups of classes with high co-occurrence frequencies. The co-occurrence probabilities of these two category groups can be found in Figure 1(b) and Figure 1(d). From the figure, we can observe that the hallucinations produced by DualPrompt often occur when the image contains one or more salient objects that strongly co-occur with the target object. For example, the *microwave* in the first image, the *oven* in the second image, and the *knife* in the fifth image. However, we must emphasize that such cases are rare in DualPrompt. In most situations, DualPrompt effectively alleviates the overfitting issue caused by label co-occurrence.

510

511
512

7 CONCLUSION

513
514
515
516
517
518
519
520
521

The paper studies on zero-shot multi-label classification using CLIP without training. We find that compared to the single-label scenarios, CLIP often obtain unfavorable performance in the multi-label scenarios due to the fact that it does not explicitly exploit co-occurrence in both pretraining and inference. To address this problem, we propose the DualPrompt method to use the discriminative prompt and correlative prompt simultaneously. The former contains the only target label, which aims to capture discriminative features, while the latter contains the target label and its co-occurring labels, which introduces co-occurrence information. Moreover, we construct a causal inference framework to provide a theoretical explanation for our method. Extensive experimental results verify the effectiveness of the proposed method.

522

523

ETHICS STATEMENT

524

This paper does not raise any ethical concerns.

526

527
528

REPRODUCIBILITY STATEMENT

529
530
531

The code of DualPrompt is available in supplementary material. The details of experimental settings are presented in Section 6.1.

532

533

REFERENCES

534
535
536
537

Ali Furkan Biten, Lluís Gómez, and Dimosthenis Karatzas. Let there be a clock on the beach: Reducing object hallucination in image captioning. In *Proceedings of the IEEE/CVF Winter Conference on Applications of Computer Vision*, pp. 1381–1390, 2022.

538
539

Tianshui Chen, Tao Pu, Hefeng Wu, Yuan Xie, and Liang Lin. Structured semantic transfer for multi-label recognition with partial labels. In *Proceedings of the AAAI conference on artificial intelligence*, volume 36, pp. 339–346, 2022.

540 Zhao-Min Chen, Xiu-Shen Wei, Peng Wang, and Yanwen Guo. Multi-label image recognition with
 541 graph convolutional networks. In *Proceedings of the IEEE/CVF conference on computer vision*
 542 and pattern recognition, pp. 5177–5186, 2019.

543

544 Zixuan Ding, Ao Wang, Hui Chen, Qiang Zhang, Pengzhang Liu, Yongjun Bao, Weipeng Yan, and
 545 Jungong Han. Exploring structured semantic prior for multi label recognition with incomplete
 546 labels. In *Proceedings of the IEEE/CVF Conference on Computer Vision and Pattern Recognition*,
 547 pp. 3398–3407, 2023.

548 Alexey Dosovitskiy, Lucas Beyer, Alexander Kolesnikov, Dirk Weissenborn, Xiaohua Zhai, Thomas
 549 Unterthiner, Mostafa Dehghani, Matthias Minderer, Georg Heigold, Sylvain Gelly, Jakob Uszkoreit,
 550 and Neil Houlsby. An image is worth 16x16 words: Transformers for image recogni-
 551 tion at scale. In *International Conference on Learning Representations*, 2021. URL <https://openreview.net/forum?id=YicbFdNTTy>.

552

553 Xiuye Gu, Tsung-Yi Lin, Weicheng Kuo, and Yin Cui. Open-vocabulary object detection via vision
 554 and language knowledge distillation. In *International Conference on Learning Representations*,
 555 2022. URL <https://openreview.net/forum?id=1L3lnMbR4WU>.

556

557 Zixian Guo, Bowen Dong, Zhilong Ji, Jinfeng Bai, Yiwen Guo, and Wangmeng Zuo. Texts as
 558 images in prompt tuning for multi-label image recognition. In *Proceedings of the IEEE/CVF*
 559 *Conference on Computer Vision and Pattern Recognition*, pp. 2808–2817, 2023.

560

561 Kaiming He, Xiangyu Zhang, Shaoqing Ren, and Jian Sun. Deep residual learning for image recog-
 562 nition. In *Proceedings of the IEEE conference on computer vision and pattern recognition*, pp.
 563 770–778, 2016.

564

565 Ping Hu, Ximeng Sun, Stan Sclaroff, and Kate Saenko. Dualcoop++: Fast and effective adaptation
 566 to multi-label recognition with limited annotations. *IEEE Transactions on Pattern Analysis and*
 567 *Machine Intelligence*, 2023.

568

569 Ranjay Krishna, Yuke Zhu, Oliver Groth, Justin Johnson, Kenji Hata, Joshua Kravitz, Stephanie
 570 Chen, Yannis Kalantidis, Li-Jia Li, David A Shamma, et al. Visual genome: Connecting lan-
 571 guage and vision using crowdsourced dense image annotations. *International journal of computer*
 572 *vision*, 123:32–73, 2017.

573

574 Jack Lanchantin, Tianlu Wang, Vicente Ordonez, and Yanjun Qi. General multi-label image classi-
 575 fication with transformers. In *Proceedings of the IEEE/CVF conference on computer vision and*
 576 *pattern recognition*, pp. 16478–16488, 2021.

577

578 Tsung-Yi Lin, Michael Maire, Serge Belongie, James Hays, Pietro Perona, Deva Ramanan, Piotr
 579 Dollár, and C Lawrence Zitnick. Microsoft coco: Common objects in context. In *Computer*
 580 *Vision–ECCV 2014: 13th European Conference, Zurich, Switzerland, September 6–12, 2014,*
 581 *Proceedings, Part V 13*, pp. 740–755. Springer, 2014.

582

583 Yuqi Lin, Minghao Chen, Wenxiao Wang, Boxi Wu, Ke Li, Binbin Lin, Haifeng Liu, and Xiaofei
 584 He. Clip is also an efficient segmenter: A text-driven approach for weakly supervised semantic
 585 segmentation. In *Proceedings of the IEEE/CVF Conference on Computer Vision and Pattern*
 586 *Recognition*, pp. 15305–15314, 2023.

587

588 Yuqi Lin, Minghao Chen, Kaipeng Zhang, Hengjia Li, Mingming Li, Zheng Yang, Dongqin Lv,
 589 Binbin Lin, Haifeng Liu, and Deng Cai. Tagclip: A local-to-global framework to enhance open-
 590 vocabulary multi-label classification of clip without training. In *Proceedings of the AAAI Confer-
 591 ence on Artificial Intelligence*, volume 38, pp. 3513–3521, 2024.

592

593 Judea Pearl. Direct and indirect effects. In *Proceedings of the Seventeenth Conference on Uncer-
 594 tainty and Artificial Intelligence*, 2001, pp. 411–420. Morgan Kaufman, 2001.

595

Alec Radford, Jong Wook Kim, Chris Hallacy, Aditya Ramesh, Gabriel Goh, Sandhini Agarwal,
 596 Girish Sastry, Amanda Askell, Pamela Mishkin, Jack Clark, et al. Learning transferable visual
 597 models from natural language supervision. In *International conference on machine learning*, pp.
 598 8748–8763. PMLR, 2021.

594 Shuai Shao, Zeming Li, Tianyuan Zhang, Chao Peng, Gang Yu, Xiangyu Zhang, Jing Li, and Jian
 595 Sun. Objects365: A large-scale, high-quality dataset for object detection. In *Proceedings of the*
 596 *IEEE/CVF international conference on computer vision*, pp. 8430–8439, 2019.

597 Ximeng Sun, Ping Hu, and Kate Saenko. Dualcoop: Fast adaptation to multi-label recognition
 598 with limited annotations. *Advances in Neural Information Processing Systems*, 35:30569–30582,
 600 2022.

601 Jiang Wang, Yi Yang, Junhua Mao, Zhiheng Huang, Chang Huang, and Wei Xu. Cnn-rnn: A
 602 unified framework for multi-label image classification. In *Proceedings of the IEEE conference on*
 603 *computer vision and pattern recognition*, pp. 2285–2294, 2016.

604 Ming-Kun Xie, Jia-Hao Xiao, Pei Peng, Gang Niu, Masashi Sugiyama, and Sheng-Jun
 605 Huang. Counterfactual reasoning for multi-label image classification via patching-based train-
 606 ing. In *Forty-first International Conference on Machine Learning*, 2024. URL <https://openreview.net/forum?id=1QIN9ZyMLz>.

609 Kaiyu Yue, Bor-Chun Chen, Jonas Geiping, Hengduo Li, Tom Goldstein, and Ser-Nam Lim. Object
 610 recognition as next token prediction. In *Proceedings of the IEEE/CVF Conference on Computer*
 611 *Vision and Pattern Recognition*, pp. 16645–16656, 2024.

612 Youcai Zhang, Xinyu Huang, Jinyu Ma, Zhaoyang Li, Zhaochuan Luo, Yanchun Xie, Yuzhuo Qin,
 613 Tong Luo, Yaqian Li, Shilong Liu, et al. Recognize anything: A strong image tagging model.
 614 In *Proceedings of the IEEE/CVF Conference on Computer Vision and Pattern Recognition*, pp.
 615 1724–1732, 2024.

616 Kaiyang Zhou, Jingkang Yang, Chen Change Loy, and Ziwei Liu. Learning to prompt for vision-
 617 language models. *International Journal of Computer Vision*, 130(9):2337–2348, 2022.

619 Qihang Zhou, Guansong Pang, Yu Tian, Shibo He, and Jiming Chen. AnomalyCLIP: Object-
 620 agnostic prompt learning for zero-shot anomaly detection. In *The Twelfth International Confer-
 621 ence on Learning Representations*, 2024. URL <https://openreview.net/forum?id=buC4E91xZE>.

623

624

625

626

627

628

629

630

631

632

633

634

635

636

637

638

639

640

641

642

643

644

645

646

647

A DERIVATION OF EQ. (2)

Considering that a correlative prompt P^c consisting of the target label L^t and its co-occurring labels L^c , let $\{L^t, L_0^c\}$ and $\{L_0^t, L^c\}$ represent two mutually exclusive events, where L_0^c (L_0^t) represents we remove the co-occurring labels (target label) from the correlative prompt. By omitting the class index k for notational simplicity, we have

$$\begin{aligned}
\mathcal{T}(\mathbf{x}) &= p(y = 1 | \mathbf{x}, L^t, L^c) - p(y = 1 | \mathbf{x}, L^c, L_0^t) \\
&= p(y = 1 | \mathbf{x}, L^t, L^c) - \frac{p(y = 1, \mathbf{x}, L^c, L_0^t)}{p(\mathbf{x}, L^c, L_0^t)} \\
&= p(y = 1 | \mathbf{x}, L^t, L^c) - \frac{p(y = 1, \mathbf{x}, L^c, L^t) - p(y = 1, \mathbf{x}, L_0^c, L^t)}{p(\mathbf{x}, L^c, L_0^t)} \\
&= p(y = 1 | \mathbf{x}, L^t, L^c) - \frac{p(y = 1 | \mathbf{x}, L^c, L^t) p(\mathbf{x}, L^c, L^t) - p(y = 1 | \mathbf{x}, L_0^c, L^t) p(\mathbf{x}, L_0^c, L^t)}{p(\mathbf{x}, L^c, L_0^t)} \\
&= (1 - \frac{p(\mathbf{x}, L^c, L^t)}{p(\mathbf{x}, L^c, L_0^t)}) p(y = 1 | \mathbf{x}, L^t, L^c) + \frac{p(\mathbf{x}, L_0^c, L^t)}{p(\mathbf{x}, L^c, L_0^t)} p(y = 1 | \mathbf{x}, L_0^c, L^t) \\
&\propto p(y = 1 | \mathbf{x}, P^c) + \lambda p(y = 1 | \mathbf{x}, P^d),
\end{aligned} \tag{3}$$

where $\lambda = \frac{p(\mathbf{x}, L_0^c, L^t)}{p(\mathbf{x}, L^c, L_0^t) - p(\mathbf{x}, L^c, L^t)}$ can be regarded as a trade-off parameter. In our experiments, we find that our method achieves favorable performance by simply setting λ to 1.

B COMPLETE RESULTS OF FIGURE 2(A)

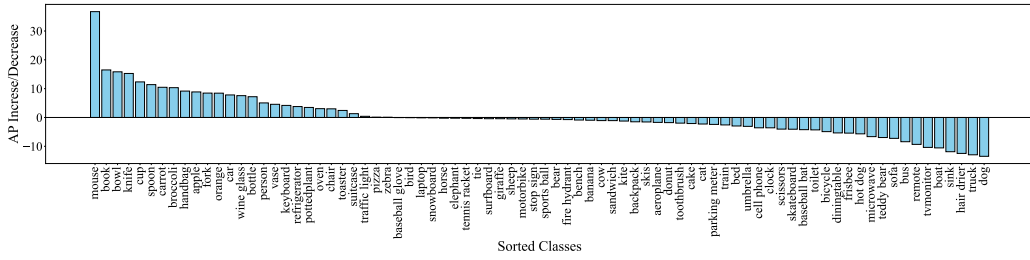


Figure 10: The performance changes of CoP against DiP in terms of AP over all cases. The performance of nearly half of the labels improved, while the performance of the other half decreased.

Figure 11 illustrates the performance changes of CoP against DiP in terms of AP over all classes. From the figure, we can see that nearly half of the labels experience performance improvements, while the other half suffer from performance declines. These results verify that co-occurrence has both good and bad effects.

C EXPERIMENTAL RESULTS ON OBJECTS365

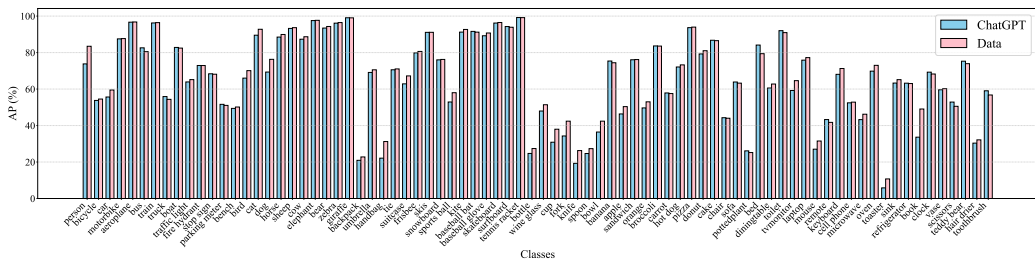
To verify that the proposed method has a broad range of applicability, we have added experimental results on a more challenging dataset, Objects365⁴ (Shao et al., 2019), which contains 365 classes. This dataset has an average of 6.17 labels per image, which is more than twice that of the COCO dataset (2.93). Table 3 reports the experimental results of our method and the comparison baselines on Objects365. For our method DualPrompt, we use 1% of the training data to estimate label

⁴<https://www.objects365.org/overview.html>

702
 703 Table 3: The comparative results between the proposed method and the state-of-the-art methods on
 704 Objects365 dataset. The best performance is highlighted in bold. Coo. Est. represents co-occurrence
 705 probabilities estimation.

	Backbone	Resolution	Training Data Usage	mAP	F1
CLIP	ResNet-101	224 × 224	None	30.0	26.8
DualPrompt	ResNet-101	224 × 224	1% Data for Coo. Est.	34.5	30.0
TagCLIP	ViT-B/16	224 × 224	None	36.7	30.4
DualPrompt + TagCLIP	ViT-B/16	224 × 224	1% Data for Coo. Est.	37.9	31.9

712
 713 co-occurrence. As shown in the table, DualPrompt significantly outperforms the baseline CLIP,
 714 achieving a 4.5% improvement in mAP. After incorporating TagCLIP, the proposed method still
 715 yields a 1.2% gain in mAP. These experimental results demonstrate the effectiveness of DualPrompt
 716 in challenging scenarios.



717
 718 Figure 11: The comparison results of DualPrompt using ChatGPT-generated co-occurrence relation-
 719 ships versus dataset-estimated co-occurrence relationships.